PAUL SCHERRER INSTITUT

PSI

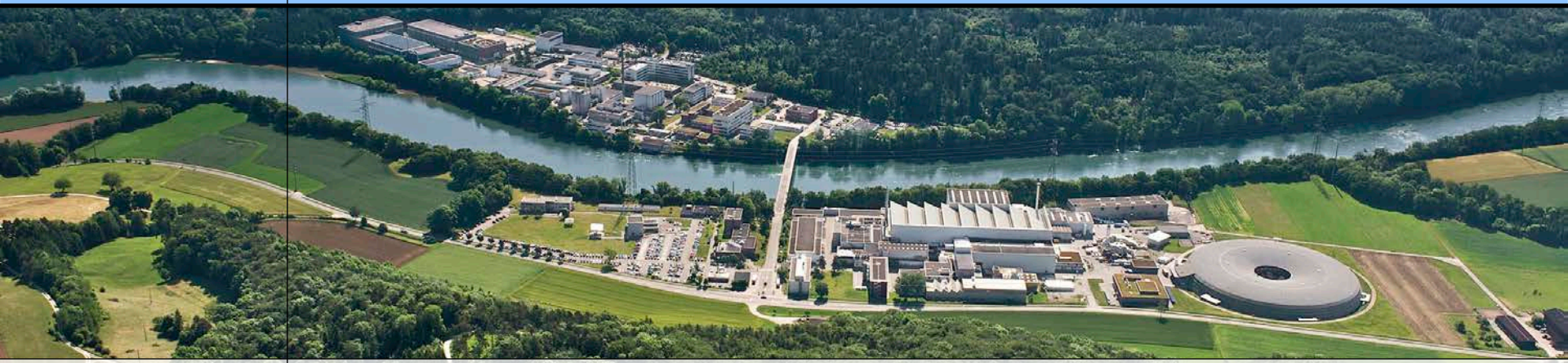

Wir schaffen Wissen – heute für morgen

Paul Scherrer Institut

4th Annual Serpent Users‘ Group Meeting (Cambridge Sept 17-19, 2014): Sandro Pelloni

Sodium void coefficient map by Serpent

Sodium void coefficient maps: Background

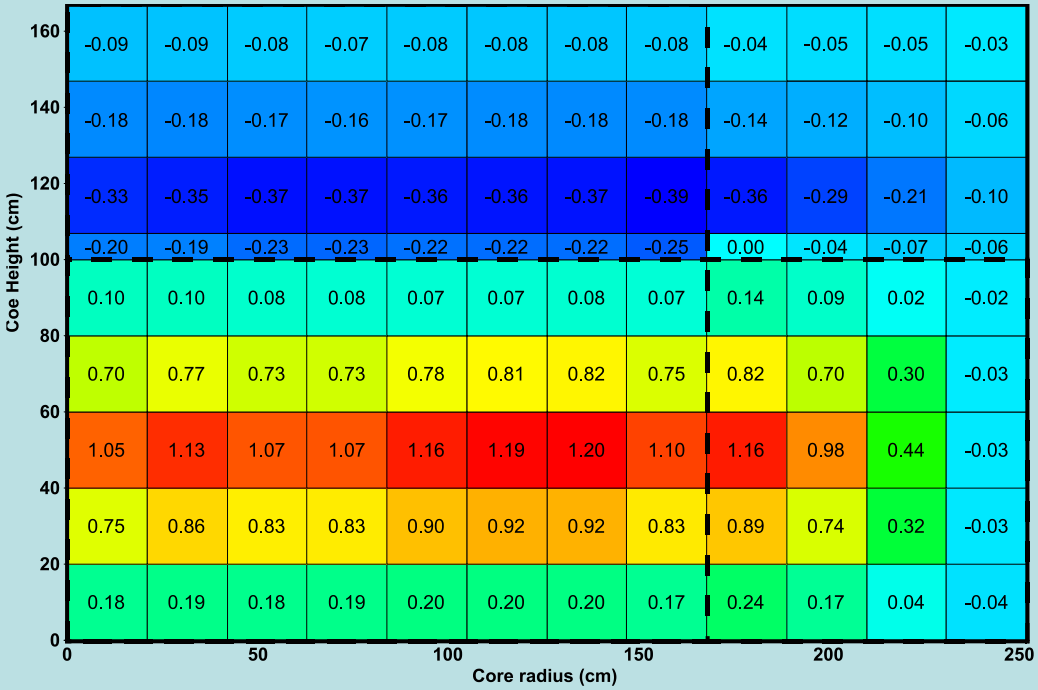

Example: Sodium void coefficient map (pcm/kg of removed Na) in ASTRID-like cores

- *Purpose: Transient analysis by means of multi-region point kinetics.*
- *Maps can be produced by means of deterministic methods (ERANOS).*
- *This study: Use of the continuous energy Monte Carlo code Serpent2 (Edition 1.15 supplied with sensitivity coefficient capabilities).*

General considerations

Use is made of the **adjoint-based k_{eff} eigenvalue sensitivity capability** as extension of the available Iterated Fission Probability Method: **POLIMI** (in collaboration with PSI and with the support of the Serpent team) by **Manuele Aufiero**.

Comparisons of the Serpent sensitivity coefficients: Agreement is achieved with ERANOS and SCALE (not part of this study).

Sensitivity coefficients: Allow to evaluate linear reactivity effects.

Stochastic approach with sensitivity coefficients:
Removes intrinsic analytical uncertainty of the sodium void coefficient associated to the use **of deterministic methods** in conjunction with systems having a large plenum.

"Complete" sensitivity coefficients (Serpent-2.1.15 extended)

$$S^{complete}_{k,\sigma^r_{x,g}} = \frac{dk/k}{d\sigma^r_{x,g}/\sigma^r_{x,g}}$$

k : Steady-state effective multiplication factor.
Regions r : Coolant channel nodes making up a **map**.

Direct term (most deterministic codes)

Indirect term

$$\frac{\partial k/k}{\partial \sigma^r_{x,g}/\sigma^r_{x,g}} + \sum_i \sum_n \sum_x \sum_j \left(\frac{\partial k/k}{\partial \sigma^{i,n}_{x,j}/\sigma^{i,n}_{x,j}} \right) \left(\frac{\partial \sigma^{i,n}_{x,j}/\sigma^{i,n}_{x,j}}{\partial \sigma^r_{x,g}/\sigma^r_{x,g}} \right)$$

$$S^{complete}_{k,\sigma^r_{x,g}} = S^{explicit}_{k,\sigma^r_{x,g}} + S^{implicit}_{k,\sigma^r_{x,g}}$$

$\sigma^r_{x,g}$: Steady-state sodium microscopic cross-section for reaction x in region r and energy group g of an arbitrary energy structure.

Reaction x: Elastic and inelastic scattering, capture and (n,xn).

$\sigma^{i,n}_{x,j}$: jth group steady-state microscopic cross-section of nuclide n for reaction x in any reactor region i. Here x also includes fission and $\bar{\upsilon}$ for fissionable nuclides.

Liner approximation: Sodium void effect and mean coefficient for full void

$$\Delta k^r = k \sum_x \sum_g S^{complete}_{k,\sigma^r_{x,g}} \frac{\Delta \Sigma^r_{x,g}}{\Sigma^r_{x,g}}$$

$$\approx k \left(\frac{N^r_{pert}}{N^r_{ref}} - 1 \right) \sum_x \sum_g S^{complete}_{k,\sigma^r_{x,g}}$$

Variation of the effective multiplication factor as a result of voiding region *r*.

$$\overline{\left(\frac{d\rho^r}{dM^r} \right)} = -\frac{1}{M^r k} \left\{ \sum_x \sum_g S^{complete}_{k,\sigma^r_{x,g}} \Big/ \left(1 - \sum_x \sum_g S^{complete}_{k,\sigma^r_{x,g}} \right) \right\}$$

Mean coefficient for full void of region *r*.

M^r : Steady-state sodium mass in region r.

$$\frac{\Delta \Sigma^r_{x,g}}{\Sigma^r_{x,g}} = \frac{N^r_{pert} \sigma^r_{x,g,pert} - N^r_{ref} \sigma^r_{x,g}}{N^r_{ref} \sigma^r_{x,g}} \approx \frac{N^r_{pert}}{N^r_{ref}} - 1$$

$\Sigma^r_{x,g} = N^r_{ref} \sigma^r_{x,g}$: Steady-state macroscopic sodium cross-section in region r and energy group g for reaction type x;

N^r_{ref}: Steady-state sodium atom number density for region r;

N^r_{pert}: Sodium atom number density for voided region r (0 for full void: boiling);

$\sigma^r_{x,g,pert}$: Microscopic sodium cross-section for voided region r and energy group g for reaction type x ($\sigma^r_{x,g,pert} \approx \sigma^r_{x,g}$).

Additional linear approximation

Variation of the effective multiplication factor e.g. as a result of fully voiding all map regions ***r*** :

$$\Delta k = -k \sum_{r} \sum_{x} \sum_{g} S^{complete}_{k,\sigma^{r}_{x,g}}$$

The individual “complete” sensitivity coefficients give each a contribution to the total effect.

Valid if the effects are also linear in space (regions ***r*** neutronically decoupled),

i.e. for central portion of the active fuel of ASTRID.

Not accurate: Non-fuel regions (plena): Leakage dominated non-linear effects.

Non-linearity in plena (PHYSOR-2014, S. Bortot et al.)

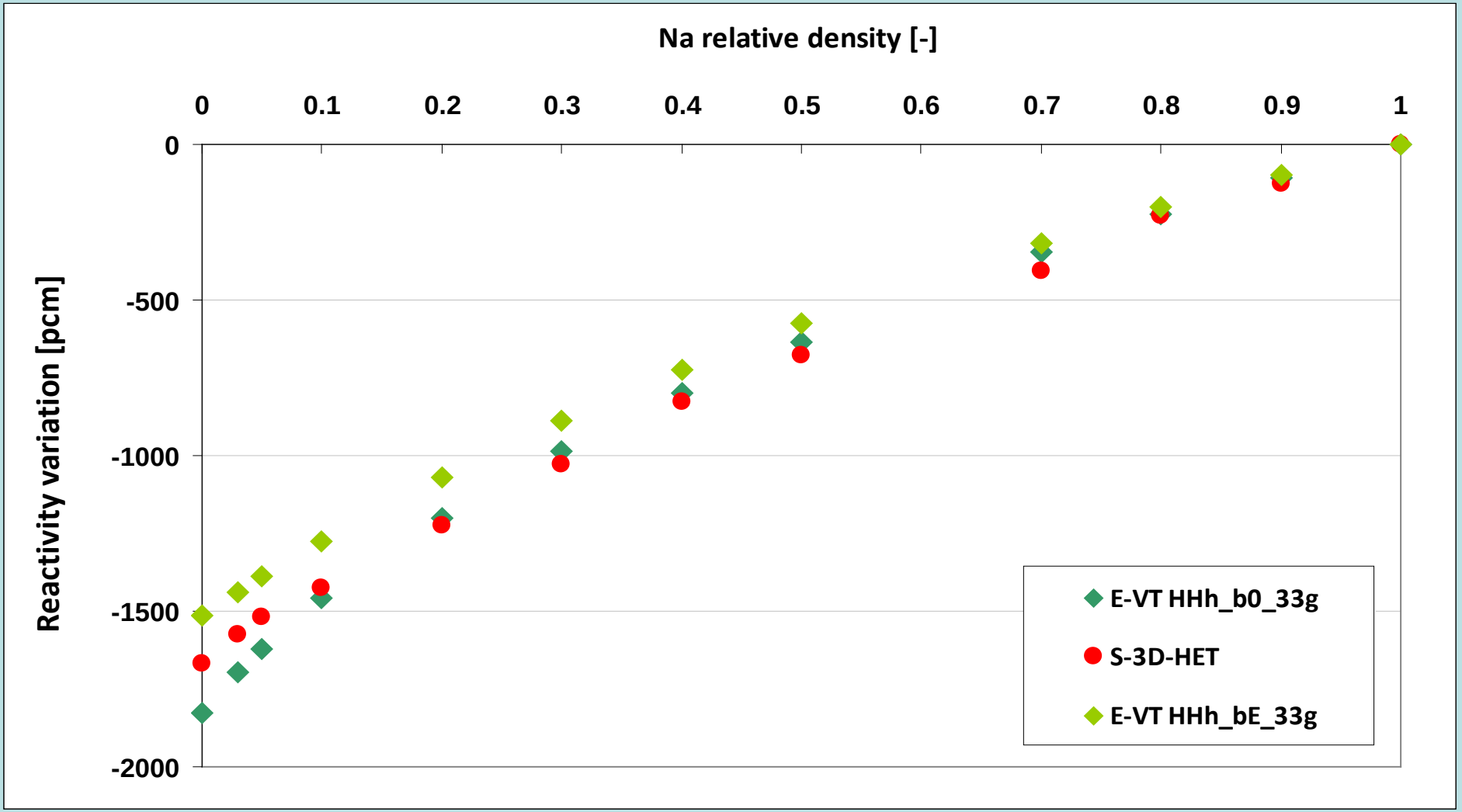

Sodium void coefficient decomposition

$$\overline{\left(\frac{d\rho^r}{dM^r}\right)} = \sum_x \sum_g \overline{\left(\frac{d\rho^r}{dM^r}\right)_{x,g}}$$

$$\overline{\left(\frac{d\rho^r}{dM^r}\right)_{x,g}} = -\frac{1}{M^r k}\left\{ S^{complete}_{k,\sigma^r_{x,g}} \Big/ \left(1 - \sum_x \sum_g S^{complete}_{k,\sigma^r_{x,g}} \right) \right\}$$

Contribution $\overline{\left(\frac{d\rho^r}{dM^r}\right)_{x,g}}$: just for **sodium** (by reaction and energy).

"Complete" sensitivity coefficient: Implicit term automatically accounts for cross-section changes additionally affecting the surroundings through enhanced neutron escape from the voided zone by larger leakage.

Leakage: Hidden in elastic scattering as for deterministic methods.

Additionally in this study: Account for non-linear effects

$\left\{ S^{complete}_{k_p,\sigma^r_{x,g}}, p = 1, \dots, N \right\}$

Partial void states p: Fractional sodium number densities of the steady-state number density in the map regions r. For convenience: Sodium density decreasing with increasing p **(piecewise linear approximation)**.

Positive sodium densities smaller than 0.74 g/cm^3 (density under the boiling point at 883^{o}C), unphysical, allowed for this purpose.

Increasing N: Reduces degree of approximation but increases computational time and numerical difficulty:

$S^{complete}_{k_{p+1},\sigma^r_{x,g}} < S^{complete}_{k_p,\sigma^r_{x,g}}$ expected due to the smaller sodium mass associated to larger p.

(Other approach, not this study: Evaluate higher order terms directly in Serpent.)

Additionally in this study: Account for non-linear effects

$$\overline{\left(\frac{d\rho^r}{dM^r}\right)} = \frac{1}{M^r}\sum_{p=1}^{N}\frac{f_p^r A_p^r}{k_p\left(1+f_p^r A_p^r\right)}$$

This approach also works for other reactivity effects e.g. Doppler.

$$f_p^r = \frac{N_{p+1}}{N_p} - 1$$

$$A_p^r = \sum_x \sum_g S^{complete}_{k_p,\sigma^r_{x,g}}$$

N_p: Sodium number density (in region r) for state p;

N_1: Normally sodium number density for steady-state ;

N_{N+1} = 0 and $f_N^r = -1$ (full void);

k_p: From Serpent (no approximation); $k_1 = k$: Normally steady state.

Linear approach: $N = 1$.

Additionally in this study: Account for non-linear effects

Detailed sodium void map: *N* (about 10) Serpent runs (as against a lot more without using sensitivity coefficients !).

Suggested number of particles per run: At least one billion.

Advantage of the stochastic approach as against deterministic methods: One energy group suffices by even easing the statistics !

Simplification: Linear approximation with **one set of "average" sensitivity coefficients** (**one Serpent run only**):

$$\overline{\left(\frac{d\rho^r}{dM^r}\right)} \approx -\frac{2}{M^r k_m}\left\{\sum_x \sum_g S^{complete}_{k_m,\sigma^r_{x,g}} \Big/ \left(1 - \sum_x \sum_g S^{complete}_{k_m,\sigma^r_{x,g}}\right)\right\}$$

***m*:** 50% void. Factor of 2: Hypothetic half mass removal.

ASTRID-like core layout (PHYSOR-2014, S. Bortot et al.)

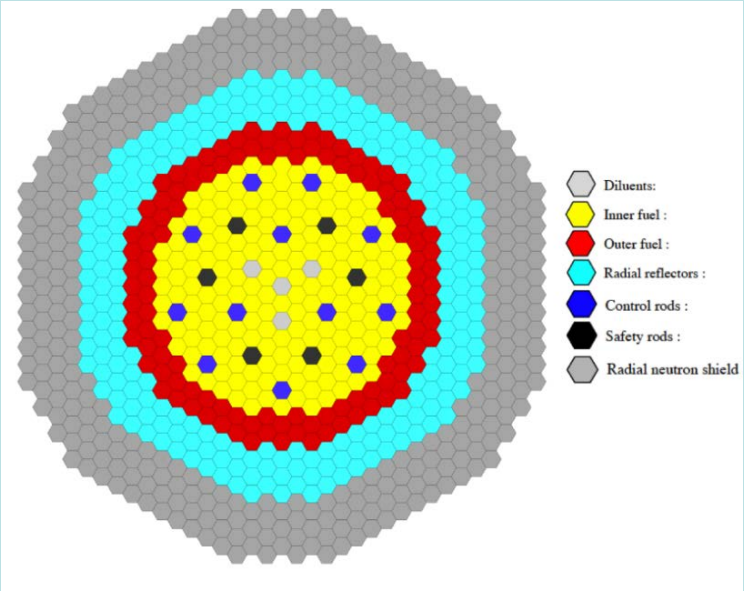

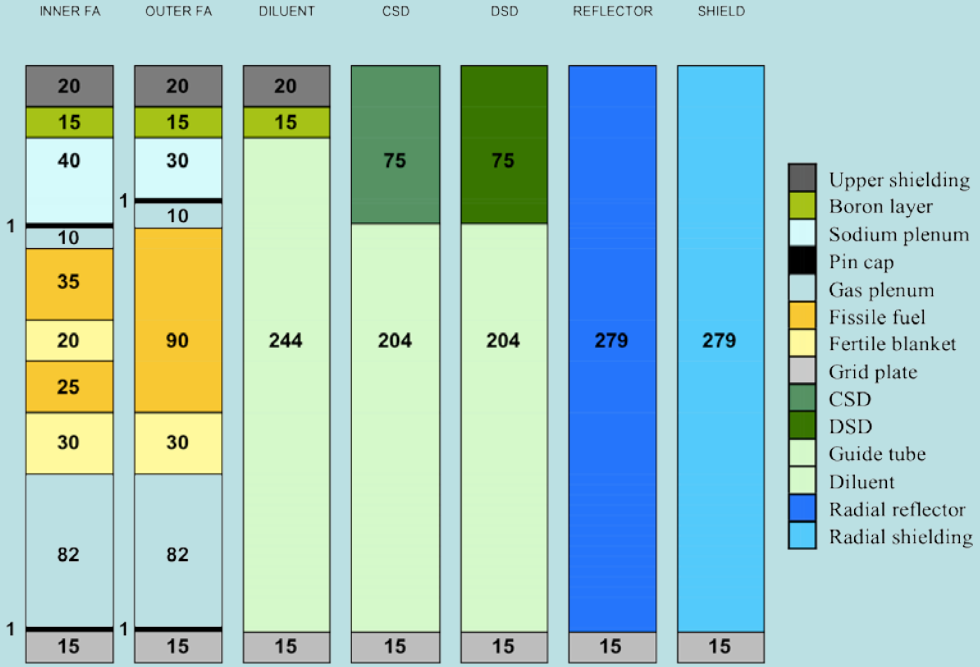

Results: Upper sodium plenum (boiling)

Void coeff.	Region below: Inner core			Region below: Outer core	
Approximate ring numbers	1-4, part of 5	Part of 5, 6	7-8	9	10
Number of fuel subassemblies	50	54	73	58	56
Axial boundaries relative to the bottom (cm)	209-224			219-234	
10^{-3}pcm/kg	-1174 *-821* *-1181* **-1132±45**	-1290 *-879* *-1296* **-1238±42**	-1351 *-889* *-1364* **-1154±31**	-618 *-433* *-609* **-539±35**	-338 *-259* *-334* **-241±41**
Axial boundaries relative to the bottom (cm)	224-249			234-249	
10^{-3}pcm/kg	-881 *-544* *-883* **-879±24**	-879 *-550* *-885* **-885±22**	-793 *-497* *-765* **-717±19**	-491 *-323* *-474* **-391±40**	-303 *-198* *-305* **-219±41**

The linear approximation is not sufficient for plena.

However, the linear approach with "average" coefficients works well.

Average regional void coefficient for **sodium plenum for the transition from steady-state to full void**

using **ten sensitivity coefficient sets for 0%, 10%, 20%, 30%, 40%, 50%, 60%, 70%, 80% and 90% void** (first line),

one sensitivity coefficient set for nominal conditions (second line), as well as

one sensitivity coefficient set for 50% void (third line);

Reference values computed by Serpent 2.1.15 with one billion particles (fourth line)

Upper sodium plenum void: Decomposition

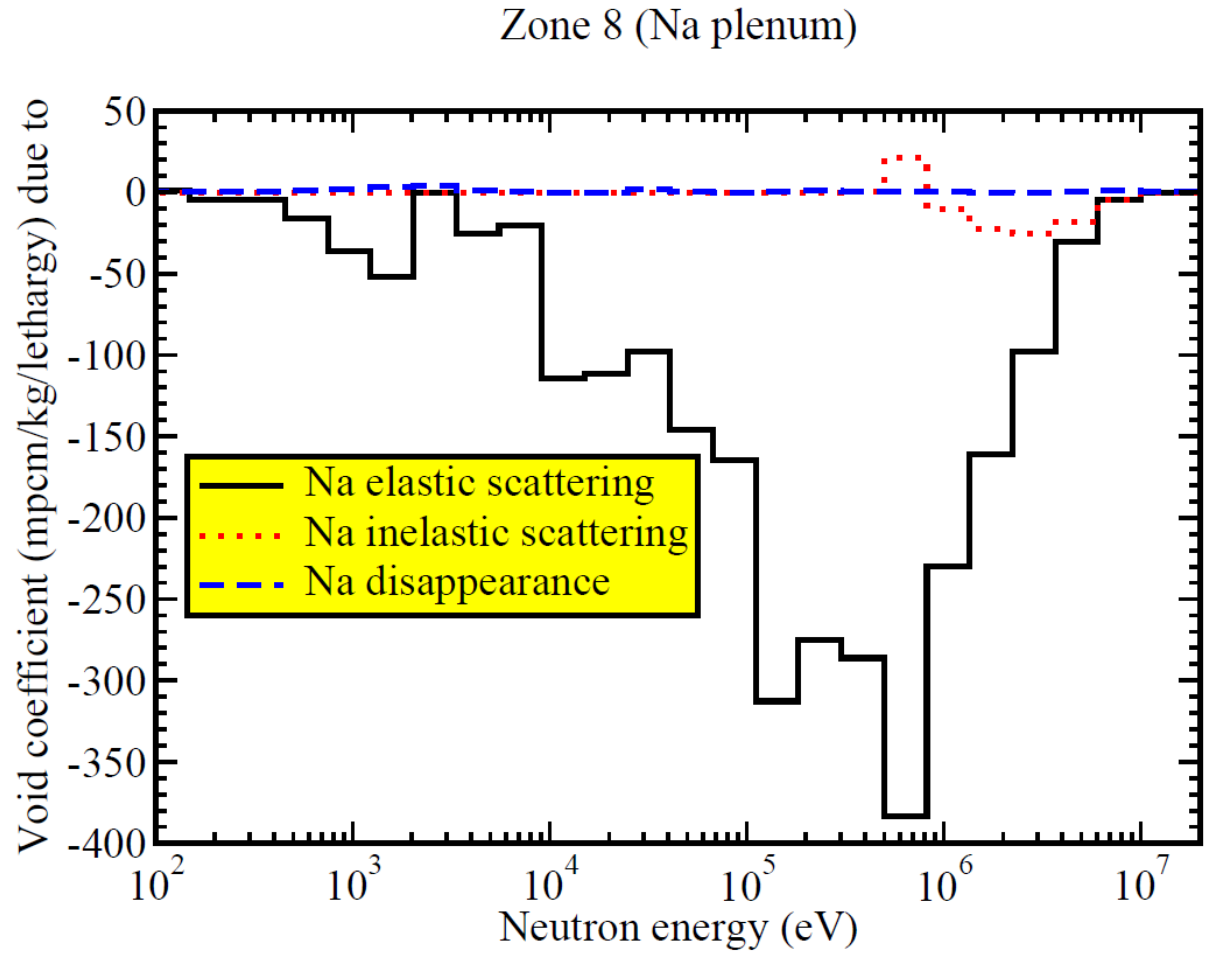

The main role of sodium elastic scattering (leakage) with a peak just below 1 MeV is shown.

Results: Upper sodium plenum (no-boiling)

Void coeff.	Region below: Inner core			Region below: Outer core	
Approximate ring numbers	1-4, part of 5	Part of 5, 6	7-8	9	10
Number of fuel subassemblies	50	54	73	58	56
Axial boundaries relative to the bottom (cm)	209-224			219-234	
10^{-3}pcm/kg	-803 *-814* *-792* **-777±200**	-891 *-872* *-910* **-785±209**	-906 *-882* *-930* **-992±137**	-446 *-430* *-463* **-520±173**	-257 *-257* *-256* **0±203**
Axial boundaries relative to the bottom (cm)	224-249			234-249	
10^{-3}pcm/kg	-570 *-540* *-601* **-792±121**	566 *-546* *-586* **-594±127**	-516 *-493* *-540* **-498±83**	-330 *-320* *-340* **-466±199**	-199 *-197* *-201* **-289±206**

The linear approximation is sufficient for plena (less non-linearity).

The void coefficient is smaller as compared to the boiling case (consistent with previous studies: The slope of the void curve is smaller).

However, since the reactivity effect is also smaller, the statistics is more difficult.

Average regional void coefficient for **sodium plenum for the transition from steady to 20% void** (thus covering the liquid phase)

using two sensitivity coefficient sets for **0%, and 10% void** (first line),

one sensitivity coefficient set for nominal conditions (second line), as well as

one sensitivity coefficient set for 10% void (third line);

Reference values computed by Serpent 2.1.15 with one billion particles (fourth line)

Results: Inner core region (boiling)

	Inner core (lower)		
Approximate ring numbers	1-4, part of 5	Part of 5, 6	7-8
Number of subassemblies	50	54	73
Axial boundaries relative to the bottom (cm)	121-133		
Average void coefficient	645 *449* *768* **326±209**	509 *476* *384*	320 *226* *310*
Axial boundaries relative to the bottom (cm)	133-146		
Average void coefficient	1548 *1346* *1528*	1646 *1608* *1659* **1503±178**	1535 *1425* *1438*
	Inner core (upper)		
Axial boundaries relative to the bottom (cm)	166-183		
Average void coefficient	2141 *1737* *2170*	2180 *1938* *2071*	2180 *1993* *2084* **2254±91**
Axial boundaries relative to the bottom (cm)	183-202		
Average void coefficient	381 *751* *389*	431 *514* *379*	376 *603* *461* **452±93**

The linear approximation is sufficient for the inner core region.

The peak value of the void coefficient in the upper part near the outer core is larger than the plenum peak value in absolute terms.

Average regional void coefficient for **inner core region for the transition from steady to full void, 10^{-3}pcm/kg,**

using ten sensitivity coefficient sets (first line),

one sensitivity coefficient set for nominal conditions (second line), as well as

one sensitivity coefficient set for 50% void (third line);

Reference values computed by Serpent 2.1.15 with one billion particles (fourth line)

Upper inner core void: Decomposition

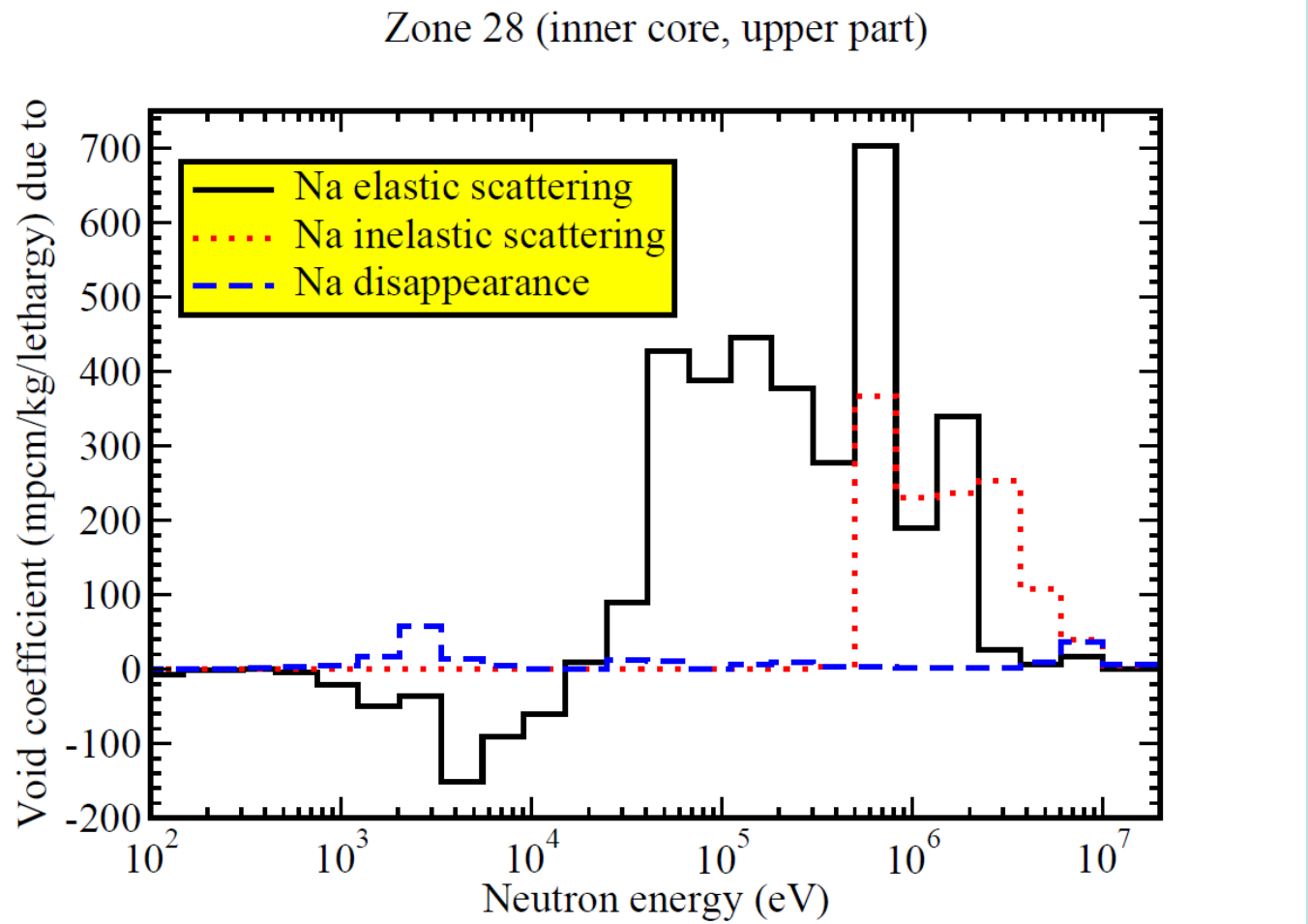

The role of sodium elastic and inelastic scattering also peaking near 1 MeV is shown.

Results: Inner core region (no-boiling)

	Inner core (lower)		
Approximate ring numbers	1-4, part of 5	Part of 5, 6	7-8
Number of subassemblies	50	54	73
Axial boundaries relative to the bottom (cm)	121-133		
Average void coefficient	449 *445* *454* **-978±1044**	444 *473* *416*	201 *224* *177*
Axial boundaries relative to the bottom (cm)	133-146		
Average void coefficient	1353 *1336* *1370*	1481 *1595* *1368* **2506±892**	1439 *1414* *1465*
	Inner core (upper)		
Axial boundaries relative to the bottom (cm)	166-183		
Average void coefficient	1915 *1723* *2108*	2058 *1930* *2194*	1965 *1977* *1954* **1531±456**
Axial boundaries relative to the bottom (cm)	183-202		
Average void coefficient	559 *745* *373*	542 *510* *574*	558 *599* *517* **73±412**

The linear approximation is sufficient for the inner core region.

The reactivity effect is smaller than for boiling, making the statistics more difficult.

Average regional void coefficient for **inner core region for the transition from steady to 20% void, 10^{-3}pcm/kg,**

using two sensitivity coefficient sets (first line),

one sensitivity coefficient set for nominal conditions (second line), as well as

one sensitivity coefficient set for 10% void (third line);

Reference values computed by Serpent 2.1.15 with one billion particles (fourth line)

Results: Outer core region (boiling)

Approximate ring number	9	10
Number of subassemblies	58	56
Axial boundaries relative to the bottom (cm)	Average void coefficient	
121-139	296 *314* *165*	-136 *-83* *-109*
139-157	1187 *1008* *1395*	88 *55* *5*
157-175	1391 *1292* *1353* **1358±121**	166 *186* *132*
175-192	957 *998* *1020*	37 *54* *82*
192-212	-181 *63* *-264*	-230 *-247* *-140* **-144±115**

The linear approximation is sufficient for the outer core region.

The peak value of the void coefficient is in the inner part.

Average regional void coefficient for **outer core region for the transition from steady to full void, 10^{-3}pcm/kg,**

using ten sensitivity coefficient sets (first line),

one sensitivity coefficient set for nominal conditions (second line), as well as

one sensitivity coefficient set for 50% void (third line);

Reference values computed by Serpent 2.1.15 with one billion particles (fourth line)

Outer core void: Decomposition

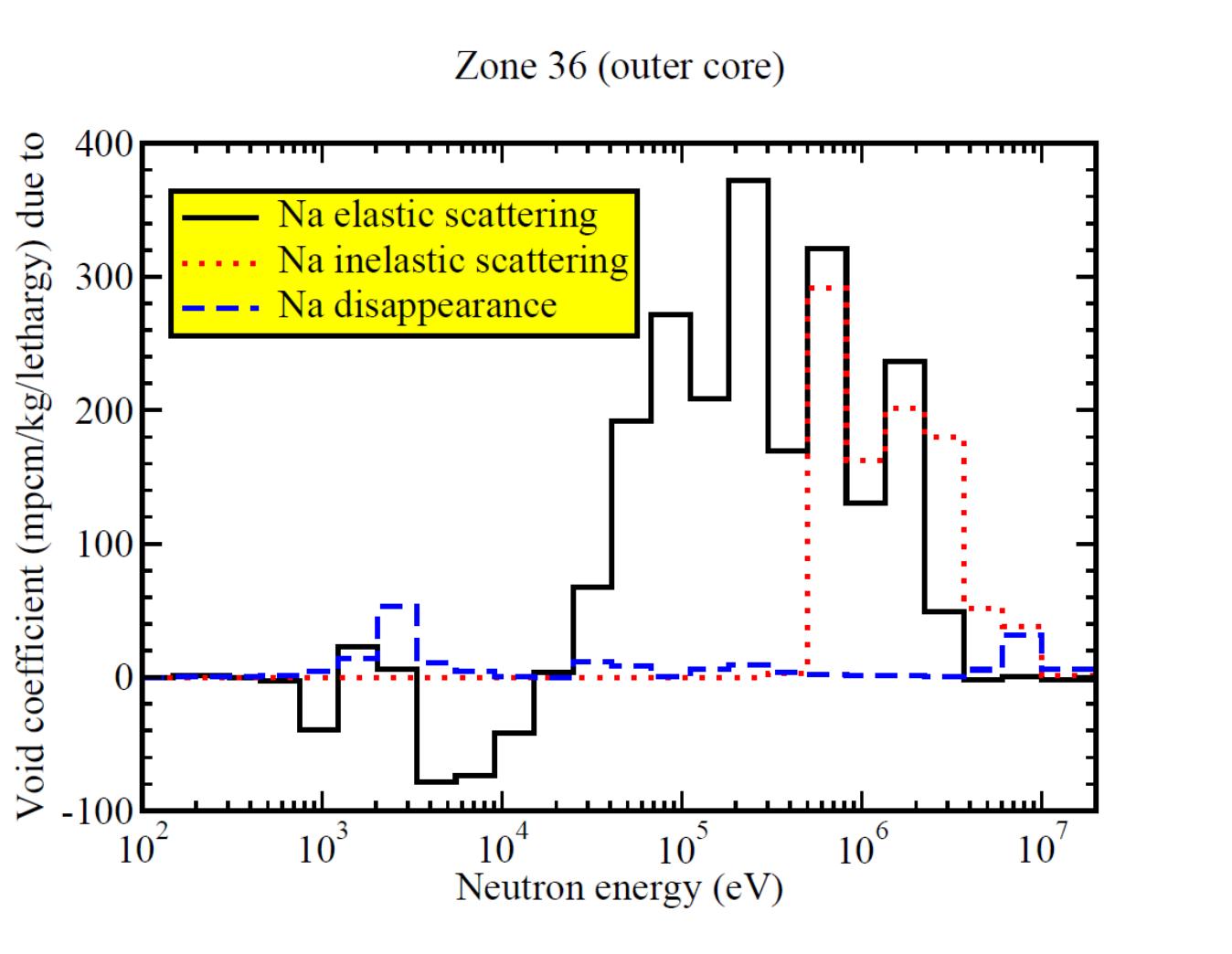

The inelastic scattering component is larger as compared to the inner core.

Results: Outer core region (no-boiling)

Approximate ring number	9	10
Number of subassemblies	58	56
Axial boundaries relative to the bottom (cm)	Average void coefficient	
121-139	251 *311* *191*	-114 *-82* *-147*
139-157	1060 *1000* *1121*	115 *55* *174*
157-175	1325 *1281* *1370* **1416±534**	184 *184* *184*
175-192	1035 *990* *1081*	44 *53* *35*
192-212	0 *62* *-62*	-252 *-245* *-259* **-180±575**

The linear approximation is sufficient for the outer core region.

The peak void coefficient value is similar to the boiling case.

Average regional void coefficient for **outer core region for the transition from steady to 20% void, 10^{-3}pcm/kg,**

using two sensitivity coefficient sets (first line),

one sensitivity coefficient set for nominal conditions (second line), as well as

one sensitivity coefficient set for 10% void (third line);

Reference values computed by Serpent 2.1.15 with one billion particles (fourth line)

Results: Inner blanket region (boiling)

	10^{-3}pcm/kg		
Approximate ring numbers	1-4, part of 5	Part of 5, 6	7-8
Number of subassemblies	50	54	73
Axial boundaries relative to the bottom (cm)	146-166		
Average void coefficient	1860 *1590* *1978*	1910 *1713* *1815* **1845±102**	1864 *1711* *1822*

The linear approximation is sufficient for the inner blanket region.

As expected, the positive coefficient is similar to the inner core region.

Average regional void coefficient for **inner blanket region for the transition from steady to full void** using ten sensitivity coefficient sets (first line),

one sensitivity coefficient set for nominal conditions (second line), as well as

one sensitivity coefficient set for 50% void (third line);

Reference values computed by Serpent 2.1.15 with one billion particles (fourth line)

Inner blanket void: Decomposition

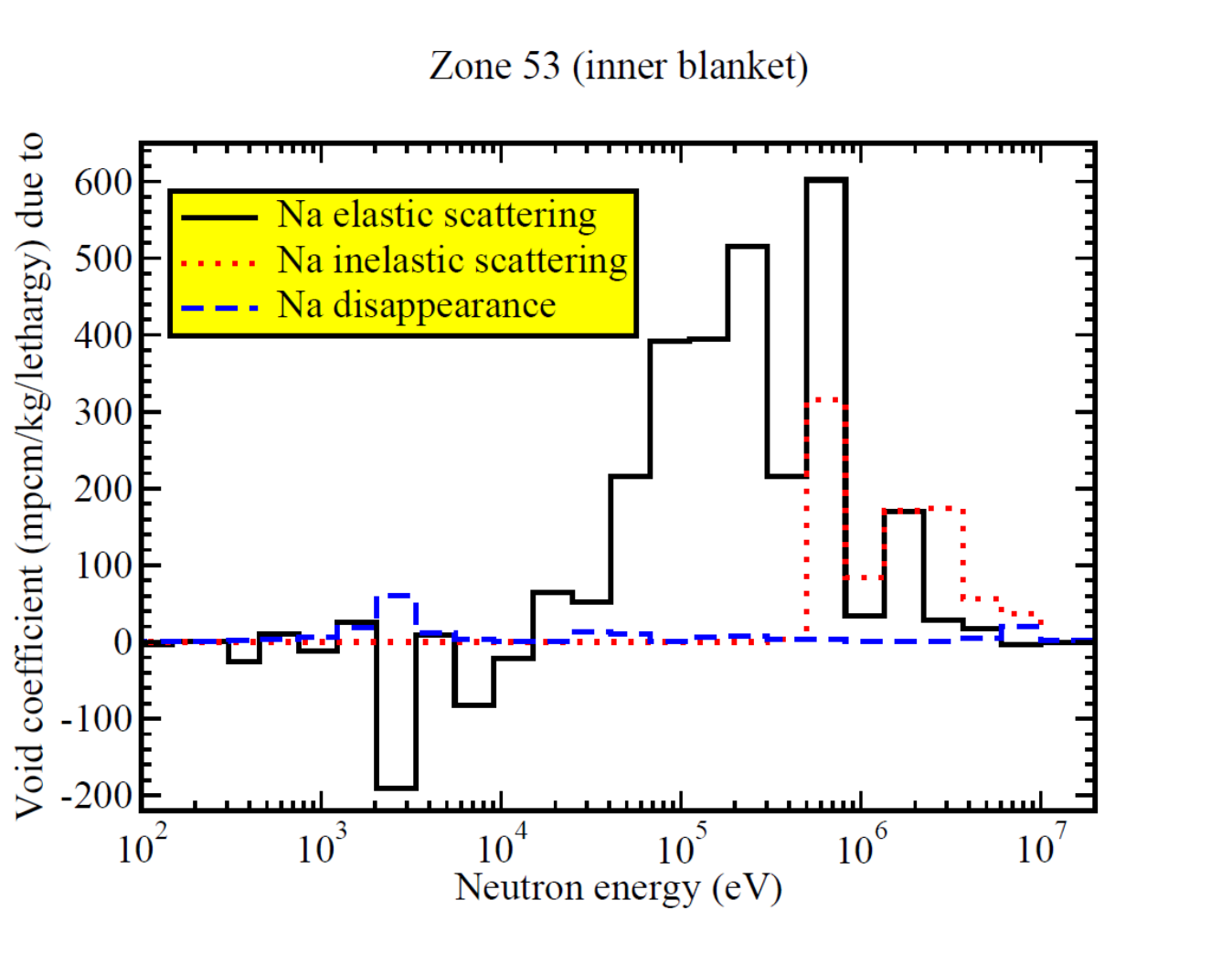

Similar to the inner core.

Results: Inner blanket region (no-boiling)

	10^{-3}pcm/kg		
Approximate ring numbers	1-4, part of 5	Part of 5, 6	7-8
Number of subassemblies	50	54	73
Axial boundaries relative to the bottom (cm)	146-166		
Average void coefficient	1586 *1577* *1595*	1670 *1699* *1641* **1358±580**	1651 *1698* *1605*

The linear approximation is sufficient for the inner blanket region.

Average regional void coefficient for **inner blanket region for the transition from steady to 20% void**

using two sensitivity coefficient sets (first line),

one sensitivity coefficient set for nominal conditions (second line), as well as

one sensitivity coefficient set for 10% void (third line);

Reference values computed by Serpent 2.1.15 with one billion particles (fourth line)

Results: Radial reflector region (boiling)

Approximate ring number	11-12	13
Number of subassemblies	134	82
Axial boundaries relative to the bottom (cm)	Average void coefficient	
0-100	-0 *0* *0*	-0 *-0* *-0*
100-200	-172 *-138* *-169* **-123±10**	-21 *-10* *-24*
200-300	-21 *-18* *-17*	-2 *-1* *-2*

Except for the "average" sensitivity coefficients, the methods overestimate the void coefficient (strong non-linearity).

However, the void coefficient is negative, but small.

Average regional void coefficient for **radial reflector region for the transition from steady to full void, 10^{-3}pcm/kg,**

using ten sensitivity coefficient sets (first line),

one sensitivity coefficient set for nominal conditions (second line), as well as

one sensitivity coefficient set for 50% void (third line);

Reference values computed by Serpent 2.1.15 with one billion particles (fourth line)

Radial reflector region void: Decomposition

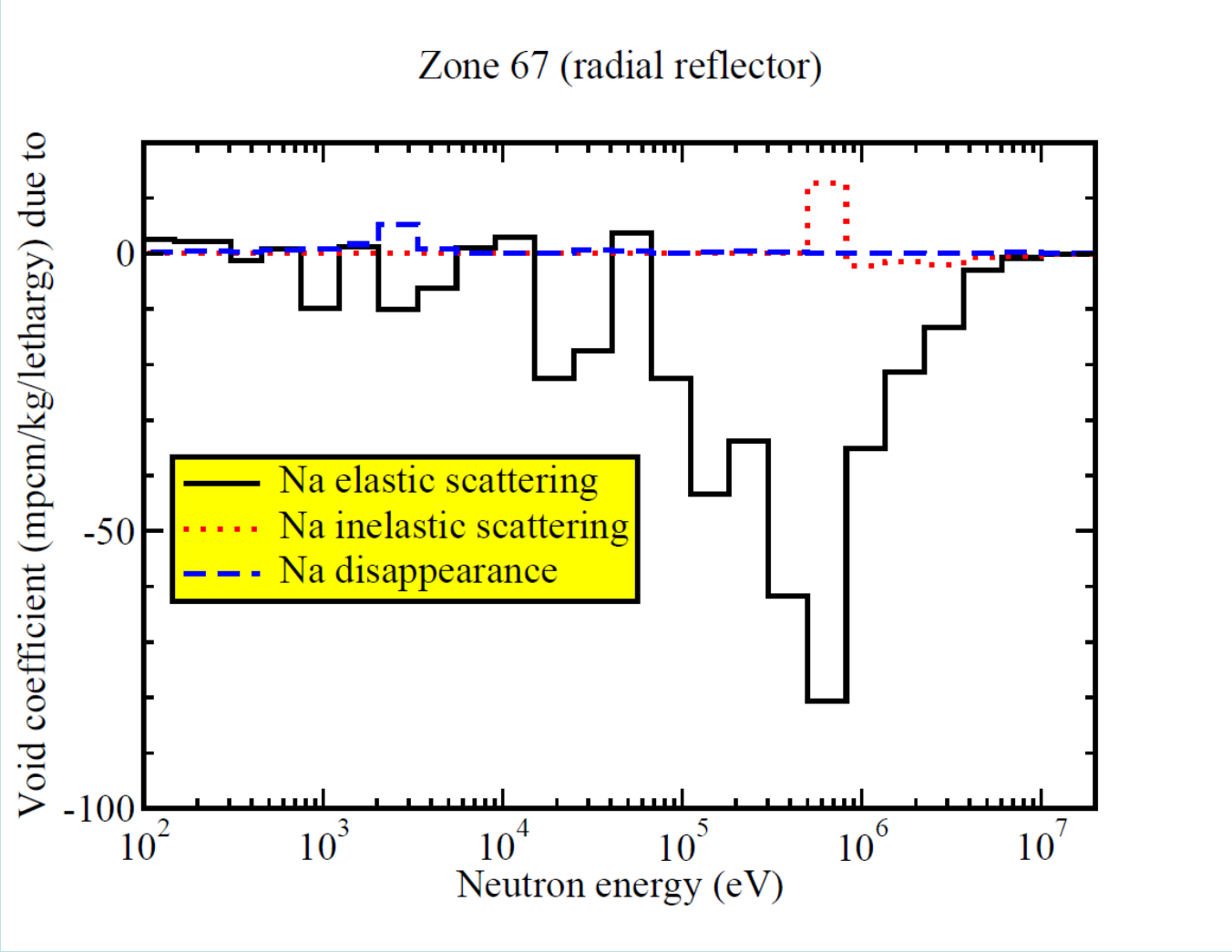

Leakage dominated.

Results: Radial reflector region (no-boiling)

Approximate ring number	11-12	13
Number of subassemblies	134	82
Axial boundaries relative to the bottom (cm)	Average void coefficient	
0-100	-0 *-0* *0*	-0 *-0* *0*
100-200	-138 *-137* *-139* **-133±50**	-11 *-10* *-13*
200-300	-19 *-18* *-19*	-1 *-1* *-1*

All methods give consistent results.

However, the statistical uncertainty is too high.

Average regional void coefficient for **radial reflector region for the transition from steady to full void, 10^{-3}pcm/kg,**

using two sensitivity coefficient sets (first line),

one sensitivity coefficient set for nominal conditions (second line), as well as

one sensitivity coefficient set for 10% void (third line);

Reference values computed by Serpent 2.1.15 with one billion particles (fourth line)

Future work

How detailed must be the map for the transient analysis?

How to include properly and to make benefit of the increased plenum coefficient when boiling?

A similar methodology will be used for other important reactivity effects such as Doppler and thermo-mechanical expansions. Thereby, use will be made of Serpent microscopic cross-sections (detector option) according to the first formula of Slide 7.

The extended version of Serpent (Edition 2.1.15)

was extensively used for assessing the sodium void coefficient in conjunction with complicated geometries.
It is then foreseen to make use of the official release of Serpent-2 with sensitivities hopefully occurring soon.

Mein Dank geht an

Manuele Aufiero, Polimi und an das ESNII+-Projektteam.